Renewable and Sustainable Energy Transition 2 (2022) 100033

Contents lists available at ScienceDirect

Renewable and Sustainable Energy Transition

journal homepage: www.journals.elsevier.com/renewable-and-sustainable-energy-transition

Full-length article

An efficient method to estimate renewable energy capacity credit at increasing regional grid penetration levels

Jethro Ssengonzi *, Jeremiah X. Johnson, Joseph F. DeCarolis

Department of Civil, Construction and Environmental Engineering, North Carolina State University, Raleigh, NC, USA

ARTICLE INFO

Keywords:
Capacity credit
Effective load carrying capability
Loss of load probability
Monte Carlo simulation

ABSTRACT

The wide scale deployment of variable renewable energy technologies (VREs) offers a pathway to decarbonize the electric grid. One challenge to reliably operating the grid is ensuring that sufficient generating capacity is available to meet demand at all hours. By determining an individual generator's contribution to resource adequacy based on its expected availability when power is needed, the capacity credit for these resources is estimated. The objective of this study is to quantify the contribution of VRE to resource adequacy as a function of VRE penetration, across several regions, technologies, and resources. A computational model was built using the effective load carrying capability (ELCC) method to calculate capacity credit values for regions spanning the contiguous United States. As the deployment of VRE increases, we show its marginal contribution to meeting peak load decreases, which in turn requires additional generating capacity to maintain reliability. In addition, a rapid approximation method is demonstrated to estimate solar and wind capacity credit, relying on the capacity factors during hours of peak net demand. We find that estimates with the lowest error relative to capacity credits calculated using the ELCC method occur using the average renewable resource capacity factors of the top net 10 demand hours, regardless of resource type. Using context-specific values for capacity credit can improve long-term decision making in generation capacity expansion, cultivating more economical long-term resource planning for deep decarbonization.

1. Introduction

Capacity credit (CC), sometimes referred to as capacity value, is a metric used to indicate an electric generator's ability to meet peak demand in a power system. Since energy demand varies daily and seasonally, accurately determining capacity credit is vital for meeting reliability standards and planning for future infrastructure investment.

Quantifying the CC for variable renewable energy technologies (VREs) poses unique challenges given the as-available nature of the resources. Wind generation varies across all hours while solar has a diurnal pattern of generation. Peak wind potential frequently occurs at night or in the early morning when load is relatively low. Solar supply tends to have a better fit with a daily load profile [1]. Both solar and wind power are impacted by location and weather patterns [2]. Solar projects can maximize CC by using favorable tilt angles and array-tracking systems that yield optimal output [3]. Additionally, the specific type of solar technology used can greatly impact CC values [4, 5]. Concentrated solar power (CSP), for example, often has higher CC than traditional photovoltaics due to the thermal inertia of CSP plants [6]. Murphy et al. assessed the role of weather/temperature change events that cause correlated generator outages, differentiating from current modeling that assumes generator failures to be independent and invariant to ambient conditions [7].

Attempts to estimate the CC for VREs have yielded differing values, but accurate determination is vital to fully understanding how demand in the electric grid can be reliably met. Balancing cost with grid reliability is key for future resource planning. If VREs are assumed to provide too little capacity credit, growth of VRE is disincentivized. If given too much credit, there is an increased risk for generation shortfalls and outages. CCs depend heavily on generator availability during the load peak period [8]. With more accurate CC calculations, better lowest cost options to maintain reliable service can be found.

The CC of variable renewables has been defined in literature as the quantity of conventional resources that could be 'replaced' by renewable production, without making the system less reliable [9]. The effective load carrying capability (ELCC), which measures equivalent firm capacity provided by a resource to maintain grid reliability, is the most common approach to determine CC, with some utilities and regulators

* Corresponding author.
E-mail addresses: jssengo@ncsu.edu (J. Ssengonzi), jjohns24@ncsu.edu (J.X. Johnson), jfdecaro@ncsu.edu (J.F. DeCarolis).

https://doi.org/10.1016/j.rset.2022.100033
Received 10 April 2022; Received in revised form 3 August 2022; Accepted 11 August 2022
Available online 14 August 2022

Table 1
Number of renewable resource clusters by region.

Region	Onshore Wind	Solar PV	Offshore Wind
NE	35	35	1
CA	5	5	1
NW	25	25	1
CEN	35	35	0
MID AT	35	35	0
N CEN	35	35	0
SE	40	40	0
SW	25	25	0
TX	5	5	0

preferring the use of the ELCC above other CC methods [10,11]. In Bromley-Dulfano et al., ELCC calculations were conducted for solar and wind in the multi-regional United States Western Interconnection with the goal of aiding policymakers and system planners in meeting decarbonization goals [12]. Kim et al. used ELCC to estimate energy storage benefits for system planning [13]. In Sodano et al., ELCC was used to determine the synergistic effects of solar and energy storage to provide capacity value [14].

In this study, previous work is expanded on by calculating the capacity credit for a wide array of solar and wind resources across the contiguous United States at a regional spatial resolution and under increasing VRE penetrations using the synthetically generated MIT Zero-emissions Electricity system Planning with HourlY operational Resolution (ZEPHYR) dataset [15]. In addition, the results estimated using the ELCC method are compared to a simple estimation method that relies on the VRE capacity factors during hours of highest net load. Both approaches could inform capacity expansion models and grid planning in a manner that reflects the dynamic nature of capacity value for wind and solar power. The advantages of utilizing an efficient CC method for effective power system planning are discussed.

2. Methods

2.1. Capacity credit calculation overview

A loss of load probability approach was used to calculate the effective load carrying capability for multiple solar and wind resources spanning nine regions covering the United States. First, a Monte Carlo simulation was conducted to estimate the distribution of generator capacity availability for each region. For given load profiles, the loss of load expectation (LOLE) was calculated, which is the number of instances demand exceeds available generation in a set time period. The loss of load probability (LOLP) was then determined, yielding the mean average of LOLE values over a set number of runs. Load was then adjusted to achieve the target reliability, allowing for the quantification of capacity provided by individual generators across regions. The ELCC was computed thereafter, defined as the amount by which a system's load can increase while maintaining the same LOLP for the grid with results specific to a particular resource deployment capacity. For renewables, ELCC is driven by the correspondence of generation during high LOLP hours.

The resulting ELCC value was divided by the nameplate capacity to determine the CC of the resource. Each of these steps is described in greater detail in the subsequent subsections, guided by the approach and equations defined in Sodano et al. [14]. Versions of this process are performed in [16,17].

The regional boundaries and input data are consistent with those used in Tools for Energy Model Optimization and Analysis (Temoa) energy system optimization model, as deployed in the current Open Energy Outlook (OEO) effort [18]. The nine regions include California (CA), Central (CEN), Mid-Atlantic (MID AT), North Central (N CEN), Northeast (NE), Northwest (NW), Southeast (SE), Southwest (SW), and Texas (TX). Types of regional energy clusters available from the MIT ZEPHYR database vary in amount, as shown by Table 1. Offshore wind resources are considered in the NE, NW, and CA regions. The wide geographical coverage follows the multi-area CC approach in [19], assuming that energy is produced and consumed in each respective region with no associated transfers from interregional transmission.

2.2. Monte-Carlo simulation for LOLP

To use the LOLP approach to evaluate the probability of a power system failing to meet load due to lack of available generation capacity, a Monte Carlo simulation is conducted to estimate the probability distribution of system-wide generator availability.

The system-wide available capacity in a given hour is determined as the sum of the available generating capacity from each plant. The grid-wide available generating capacity sum for each region is determined as described in Eq. (1).

$$G_t = \sum_{i \in I} g_{it} e_{it}, \ \ \forall t \in T \tag{1}$$

Equivalent forced outage rates during times of demand (EFORd) for each dispatchable generator are compared against random numbers to determine each electric generating unit's availability for a given simulation (as defined by Eqs. (2a) and (2b)). In each simulation, a random number r_i between zero and one is selected to determine the value of e_i for each existing non-renewable dispatchable unit, as follows:

$$\begin{cases} If \ r_i < (1 - EFORd), \ then \ e_i = 1 \\ \qquad otherwise \ e_i = 0 \end{cases} \tag{2a}$$

$$\begin{cases} If \ r_i > EFORd, \ then \ e_i = 1 \\ \qquad otherwise \ e_i = 0 \end{cases} \tag{2b}$$

whereby $e_i = 1$ means a generating plant is online and $e_i = 0$ means a generating plant is offline. The EFORd value represents the probability that the generator will be unavailable due to a forced outage or derating during a time when there is demand for this generator. Most forced outage rates are less than 10%, but some plant types have much higher EFORd values. Generators with higher forced outage rates typically have lower ELCC values relative to their respective rated capacity. These outages require power systems to build adequate reserve margins to ensure reliability in instances of high demand and or when a considerable share of generation is under forced outage [20].

Like in studies from [6] and [21], 2018 North American Electric Reliability Corporation (NERC) EFORd values by generator type are utilized [22]. For all generators above 25 MW in each region, generator nameplate capacities are obtained from PowerGenome with inputs that were tailored to be used in the OEO [18]. Projected 2020 hourly demand data from PowerGenome [23] formulated by data from primary sources such as the U.S. Energy Information Administration (EIA) is also used [24].

2.3. LOLP calculation and baseline adjustment

To determine the ELCC, the LOLP approach was used with the Monte Carlo distribution data. The cumulative available generation results (G_t) are compared to the net load values for every hour of the year, represented as L_t (defined by Eq. (3)). If there is an instance where G_t is less than L_t, the binary variable d_t is set to 1 to represent a loss of load event. Otherwise, d_t is equal to 0.

$$\begin{cases} If \ G_t < L_t, \ then \ d_t = 1 \\ \quad otherwise \ d_t = 0 \end{cases} \tag{3}$$

LOLE can be interpreted as the sum of outage hours over the course of a time period T when demand exceeds generation divided by the total number of hours in that selected time period [21]. The most common

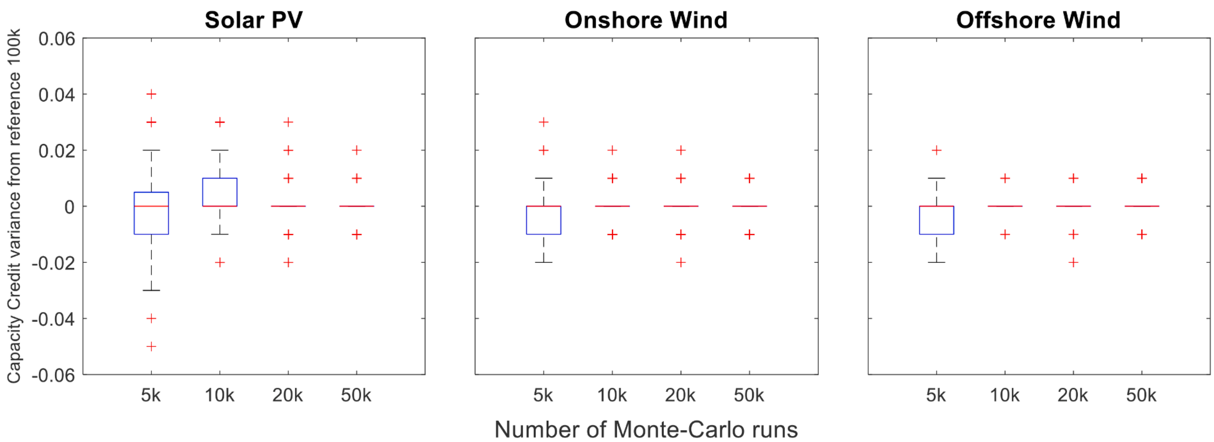

Fig. 1. Capacity credit variance by number of Monte Carlo samples for aggregated variable renewable energy resources in the Northeast and Texas.

selected time period is the 8760 h of the year planning horizon. The resulting quotient is shown in Eqs. (4a) and (4b):

$$LOLE = \frac{\sum_{t=1}^{T} d_t}{T}, \ or \tag{4a}$$

$$LOLE = \sum_{t=1}^{T} p\{G_t < L_t\} \tag{4b}$$

LOLE is calculated for every iteration j of the available generation values across all modeled hours of demand.

The LOLP approach is used to evaluate the probability of a power system failing to meet load due to lack of available generation capacity in a given time period [21]. LOLP for each trial k can be described using Eq. (5):

$$LOLP_k = \frac{1}{n} \sum_{j=1}^{n} LOLE_{j,k} \tag{5}$$

The assumed standard desired LOLP for operating utilities in this study is 24 h of outage every 10 years (approximately 2.7397×10^{-4}), which is a common reliability target in the United States and in Europe [2,20]. This benchmark reliability is used to establish a reserve generation margin that seeks to balance the competing goals of reliability and avoiding the construction of costly excess generation capacity. The selected LOLP is only one of several benchmark reliability targets used in the resource adequacy modeling space [7]. As discussed in Murphy et al., targets can range from one loss of load event every 50 years to nearly one loss of load event every 5 years. This reliability can be equated to establishing an adequate planning reserve margin [25].

2.4. ELCC and capacity credit calculation

Calculation of LOLP is vital to determining the useful metrics of ELCC and capacity credit. For all existing time periods in analysis and each trial k,

$$\begin{cases} If \ G_{t,k} + G_{newVRE,t} \ < \ L_t + L_k + L_s, \ then \ d'_{t,k} = 1 \\ \qquad otherwise \ d'_{t,k} = 0 \end{cases} \tag{6}$$

where $G_{newVRE,t}$ are incremental amounts of new VRE capacity, and L_s is additional fixed load added to the grid to determine the updated binary variable $d'_{t,k}$. Before new VRE resource is accounted for, cumulative available generation of a trial $G_{t,k}$ is compared to the sum of the existing net load value to the grid L_t and the fixed load adjustment to reach desired baseline grid reliability L_k. The L_t includes dispatchable non-renewable plants and existing VRE plants that are treated as negative load. After all existing capacity is accounted for, new renewable resource $G_{newVRE,t}$ is added as a negative load and the additional fixed load L_s is added to return the grid the desired reliability level (as defined by Eq. (6)). This LOLP process is shown in Eqs. (7a) and (7b), an expansion of Eq. (5) to include L_k, $G_{newVRE,t}$, and L_s.

$$LOLP_k = \frac{1}{n} \sum_{j=1}^{n} \frac{\sum_{t=1}^{T} d'_{t,k}}{T}, \ or \tag{7a}$$

$$LOLP_k = \frac{1}{n} \sum_{j=1}^{n} \sum_{t=1}^{T} p\{G_{t,k} + G_{newVRE,t} \ < \ L_t + L_k + L_s\} \tag{7b}$$

Incremental amounts of VRE are added to the grid to reduce net load in each hour, thus potentially decreasing the present LOLP and improving power system reliability. After obtaining an initial LOLP of a region, the amount of demand that needs to be added or subtracted uniformly across all hours to converge to the desired LOLP is calculated (i.e., to adjust for overbuilt or underbuilt power systems). The process is used for each region independently [19]. To then calculate the ELCC, additional fixed load L_s is added to every hour at a value that increases the system outages to the desired LOLP benchmark. The L_s result represents the ELCC, defined as the amount of additional load the system can reliably serve in response to the addition of VRE generation. Dividing this value by the nameplate capacity $G_{s,nameplate}$ of the technology provides its capacity credit CC_s, as shown in Eq. (8).

$$CC_S = \frac{L_s}{G_{s,nameplate}} \times 100\% \tag{8}$$

A constraint is implemented to ensure that the added VRE does not bring the net demand below zero. If the VRE generation applied exceeds the demand, the net demand $L_{Net,t}$ at that hour is considered to be zero, with additional renewable generation curtailed. These load balancing constraints are represented in Eqs. (9) & (10).

$$L_{Net,t} = L_t + L_k + L_s \tag{9}$$

$$\begin{cases} If \ G_{newVRE,t} \ > \ L_{Net,t}, \ then \ L_{Net,t} = 0 \\ otherwise \ L_{Net,t} \ = \ L_t + L_k + L_s - \ G_{newVRE,t} \end{cases} \tag{10}$$

CC is calculated multiple times for each resource, each time increasing the penetration of that $G_{newVRE,t}$ resource by 1000 MW. To be able to accurately calculate and detect changes in CC, an L_s step size of 10 MW is utilized. These 10 MW L_s are added until the grid LOLP converges back to the desired reliability standard, thus yielding CC results at a resolution size of 1%. This increment choice balances computational tractability with precision of results.

The ELCC method used to determine CC can yield a full range of operating conditions but with increased computational cost [8]. Having a method to estimate CC with little computational time is valuable. As

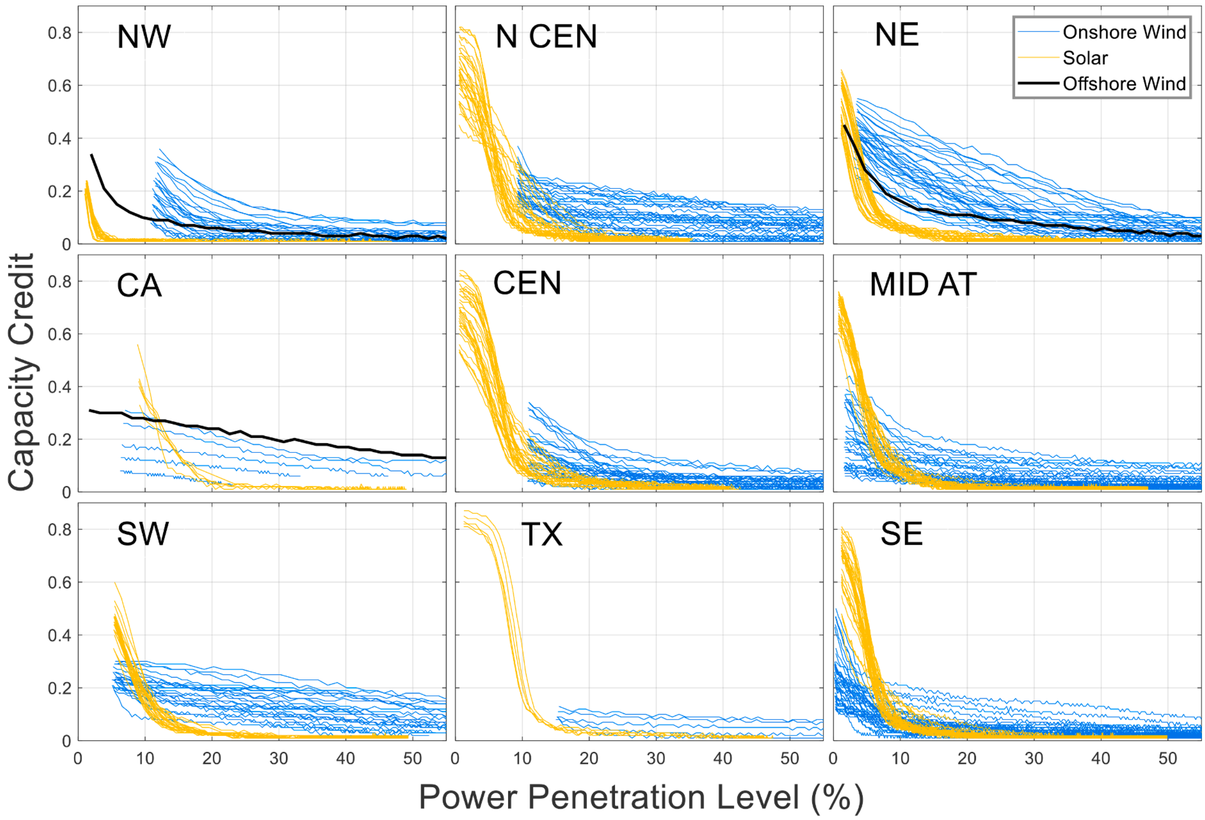

Fig. 2. Regional capacity credit for new onshore wind, offshore wind, and solar power, as a function of penetration levels.

seen in capacity factor-based methods in [6], there is evidence that average capacity factor has correlation with CC under certain conditions. To estimate CC with much less computational intensity, curves for the average renewable resource capacity factor from the top net demand hours for each resource cluster are developed in each region under increasing VRE penetration to compare to the ELCC-derived CC curves.

3. Results

3.1. Statistical analysis of Monte-Carlo trials

A statistical analysis was completed to determine a suitable number of available capacity simulations that would capture potential extremes of several plants being online or offline in a given hour. In Sodano et al., 50,000 simulations were used [14]. Other studies have relied on 1,000 to 10,000 Monte Carlo runs [26,27] such as in Bromley-Dulfano et al. where 5,000 Monte Carlo runs were used [12]. Here, CCs for thirty 1000-MW increments of new VRE are tested for two case study regions of NE and TX with ranging Monte-Carlo samples from 5,000 to 100,000. Fig. 1 displays aggregated boxplots for the resource clusters with results compared to those found under 100,000 Monte Carlo simulations.

The results in Fig. 1 show that using 10,000 Monte Carlo simulations yields little difference in results, when compared to 100,000 Monte Carlo simulations, when viewed collectively across the NE and TX regions. When aggregating data between NE and TX by resource type, the variance in CC is no more than $\pm$ 0.05 from the reference 100,000 Monte Carlo runs. As such, for this study, 10,000 Monte Carlo runs were used in the determination of ELCC.

3.2. Regional capacity credit curves

The ELCC calculation process is repeated under increasing penetrations of solar and wind power to provide insights into the incremental capacity credits for VREs. Fig. 2 displays changes in CC with gradual increase in resource grid penetration, where penetration level is the percentage of demand met by the selected VRE resource in every hour over the course of a year. Several curves start beyond the 0% power penetration level due to existing VRE capacity already being present. 240 onshore wind resources, 240 solar resources, and 3 offshore wind resources across nine regions spanning the contiguous United States are evaluated.

An increasing share of VRE consistently leads to decreasing firm capacity contributions. This result holds true across all regions examined. The curves in Fig. 2 display a similar behavior displayed by CC curves in [2,20]. Heterogeneity is observed in the magnitude of the CCs across different renewable resource in each region, highlighting the geographical sensitivity of the metric.

Common trends for technologies across the regions were observed. Solar power tends to have high CC at low penetration levels, but quickly decreases when 10 to 20% of generation is met with solar, as also shown in [3,28]. Onshore wind capacity typically starts out at a much lower CC than solar power but declines at a lower rate when compared to solar. Offshore wind tends to perform similarly to solar in the tested scenarios. This behavior could possibly be attributed to sea breezes being fueled by coastal temperature gradients, which result in better correspondence to peak load when compared to onshore wind resources; given the limited input data for the resource type however, comprehensive takeaways from the performance of offshore wind are inconclusive. Increasing VRE penetration decreases the net load peak at hours of that generation, eventually pushing the new net load peak to hours with little VRE generation, thus decreasing the capacity credit of the next increments.

Previous studies for utilities and system planners have assumed static VRE CCs [9], but our results demonstrate that this benefit cannot be assumed to be constant all the time. As found in [29], it is evident that there is a relationship between CC and penetration level for all types of generation, including non-renewables. In scenarios where baselining is

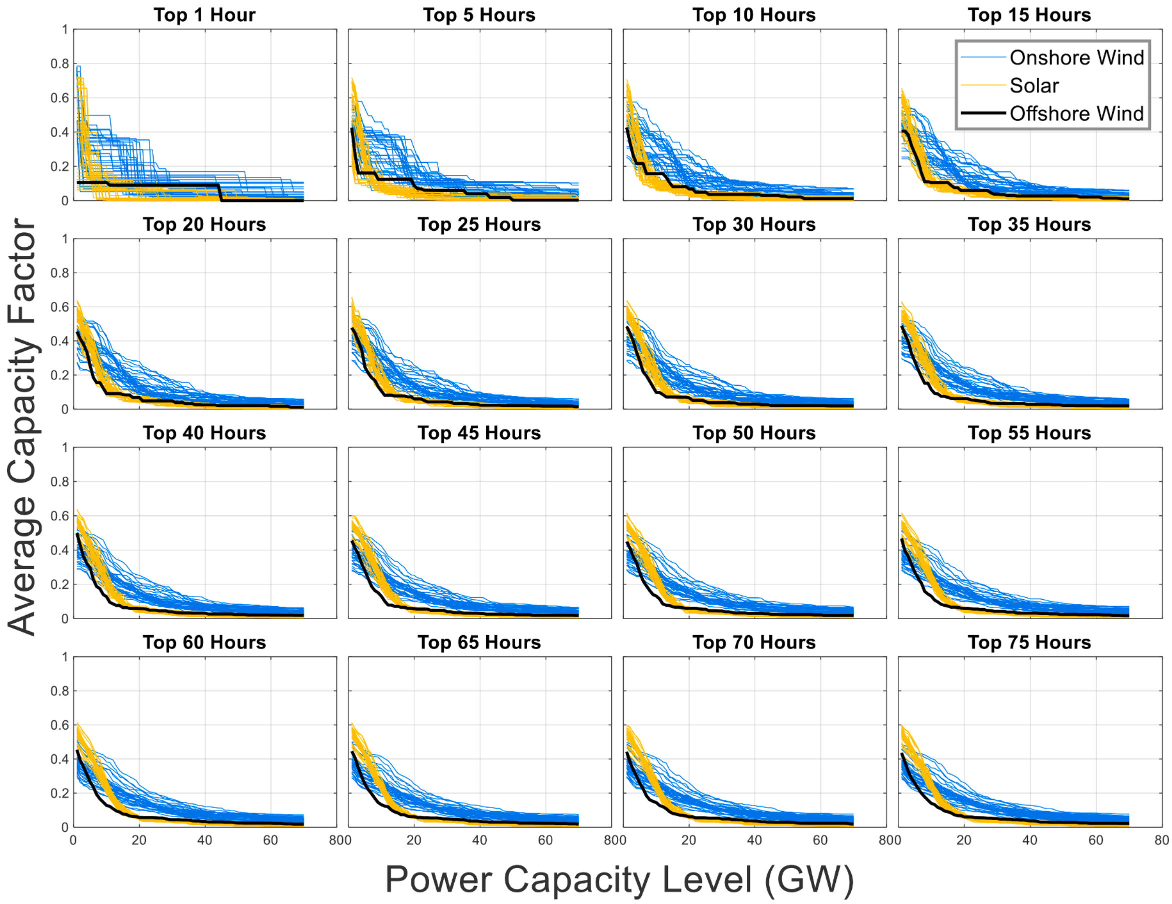

Fig. 3. Average capacity factor for wind and solar power during highest net load under increasing renewable capacity, NE.

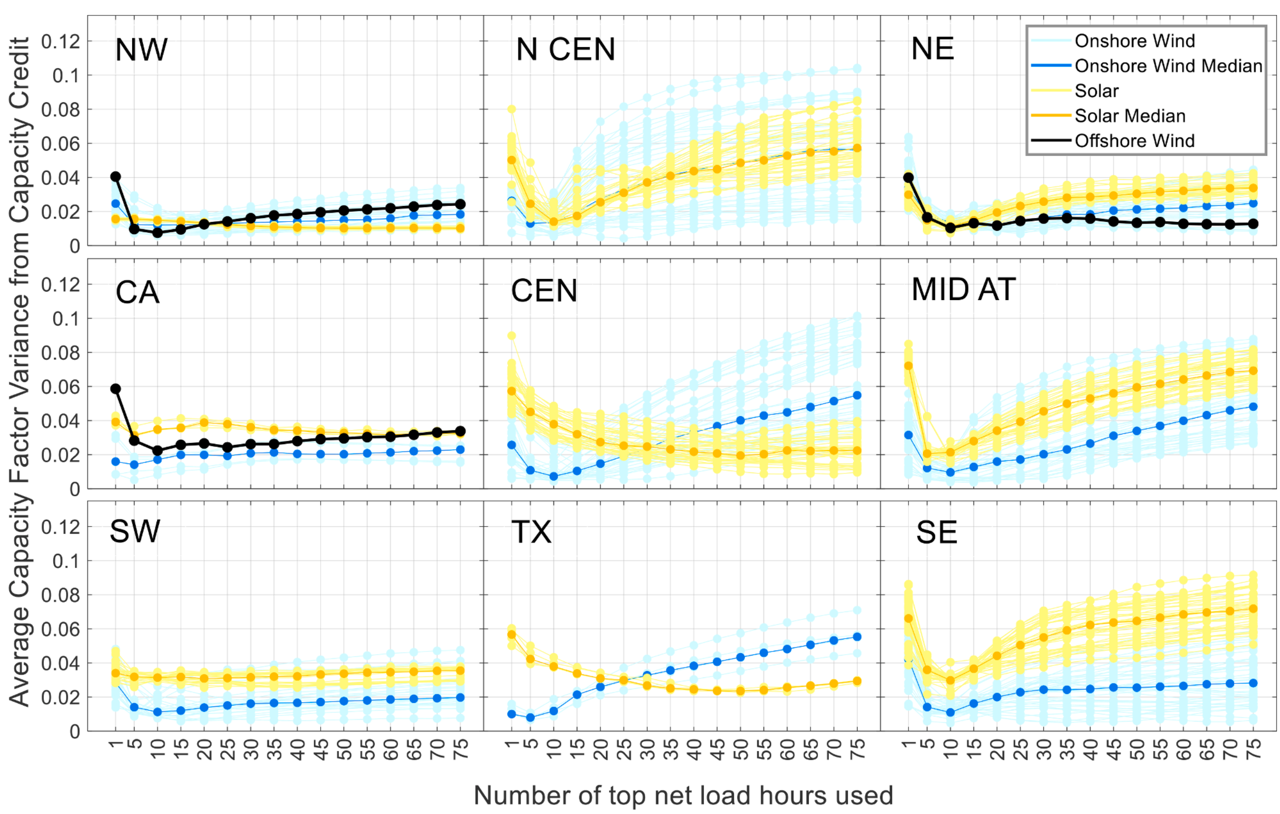

Fig. 4. Variance of resource clusters capacity factor estimation under a range of peak net load hours, all regions.

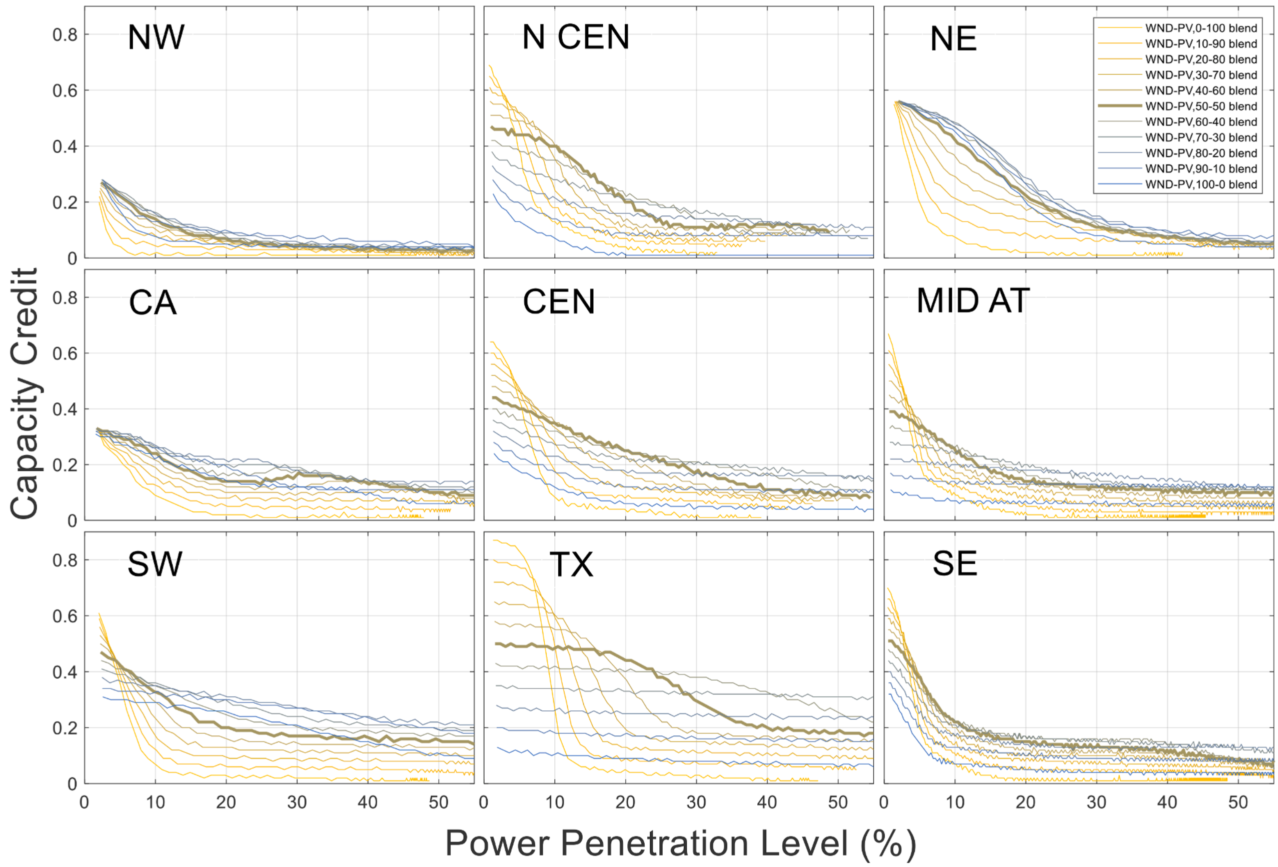

Fig. 5. Capacity credit curves for various WND-PV blends by percentage, all regions.

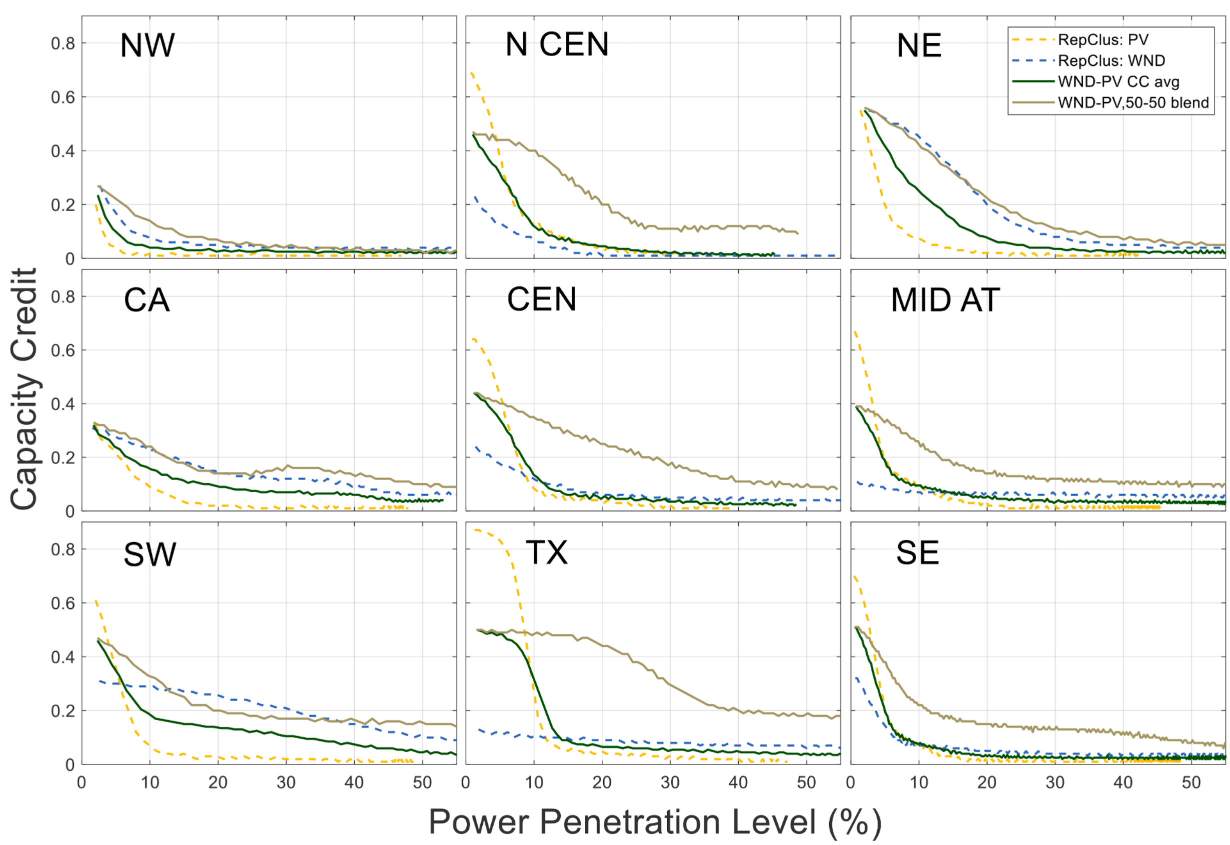

Fig. 6. Average of individual WND and PV resource CCs compared to 50-50 WND-PV blend CC, all regions.

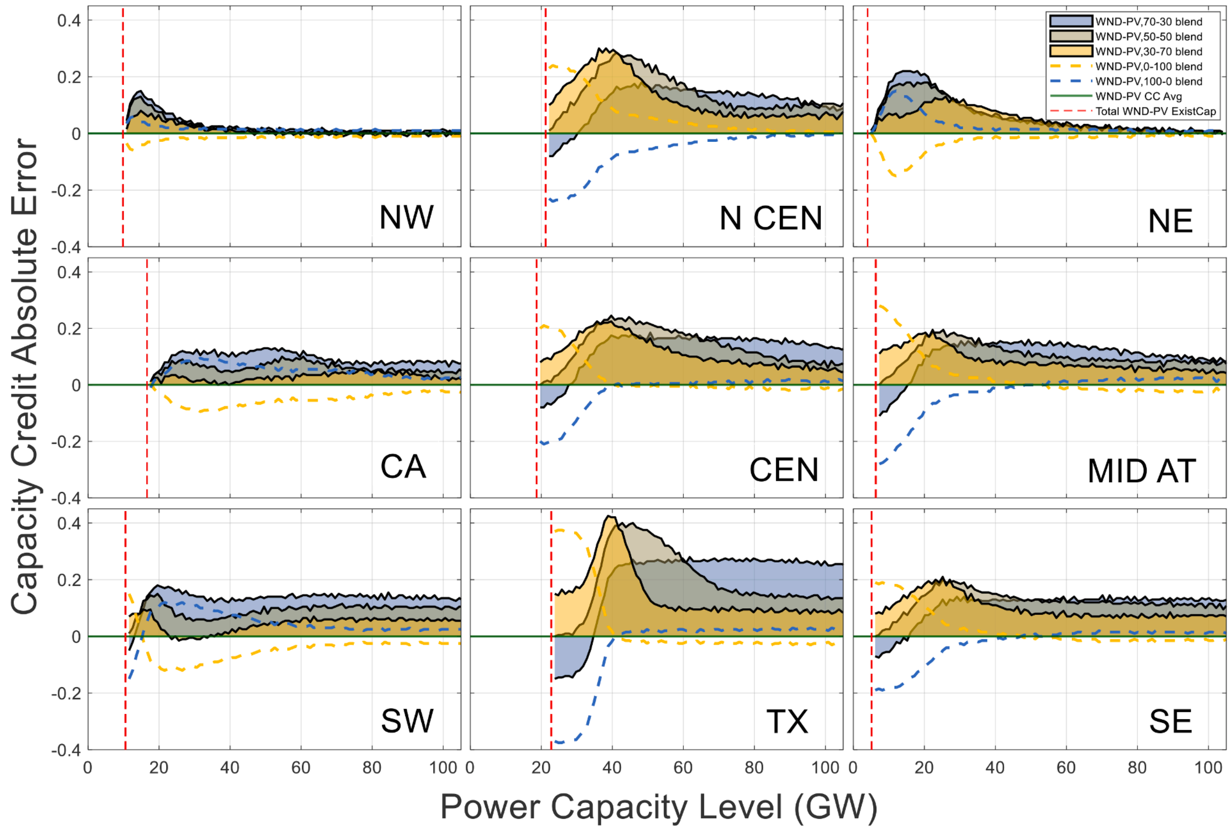

Fig. 7. Absolute error for blend mixes with respect to WND-PV CC average, all regions.

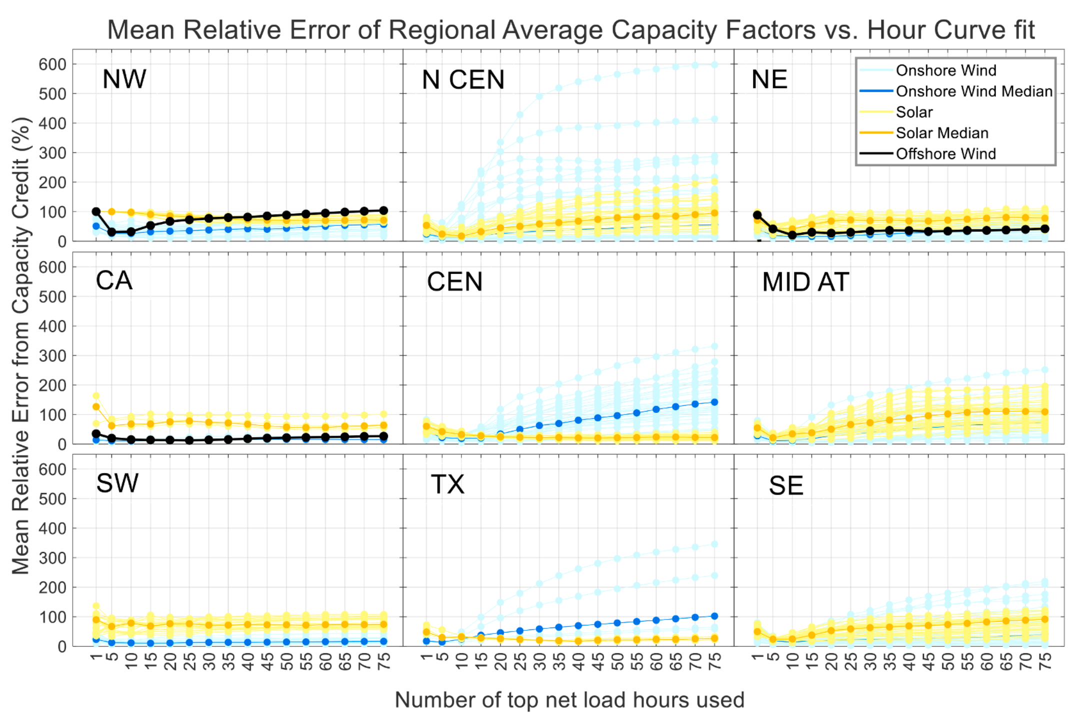

Fig. A1. Mean relative error of resource clusters capacity factor estimation under a range of peak net load hours.

not done, generating units added to a high LOLP grid will have a higher CC at a given penetration level [8]. For VREs in particular, the penetration level of the technology will play a large role in the magnitude of the capacity provided by the next increment of the resource [4].

3.3. Simple capacity credit estimation method

The calculation of the ELCC values for each region at each penetration level is a time and computationally intensive process. In this section, the accuracy of a simple estimation method that relies solely on

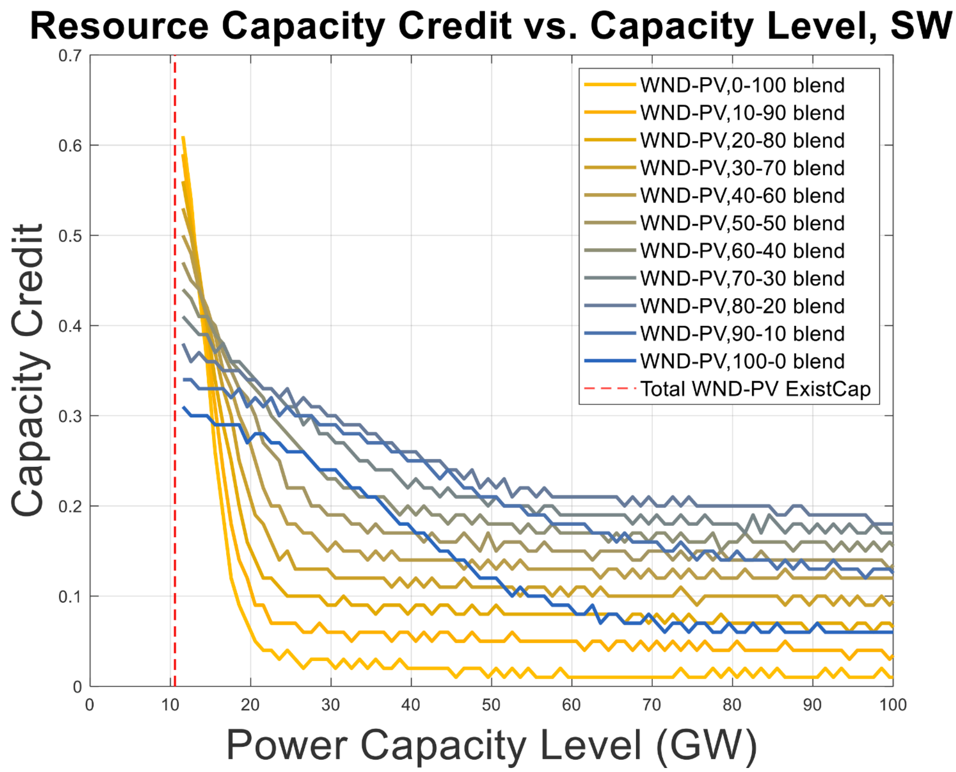

Fig. A2. Various onshore wind and solar resource mix blends from representative clusters, SW.

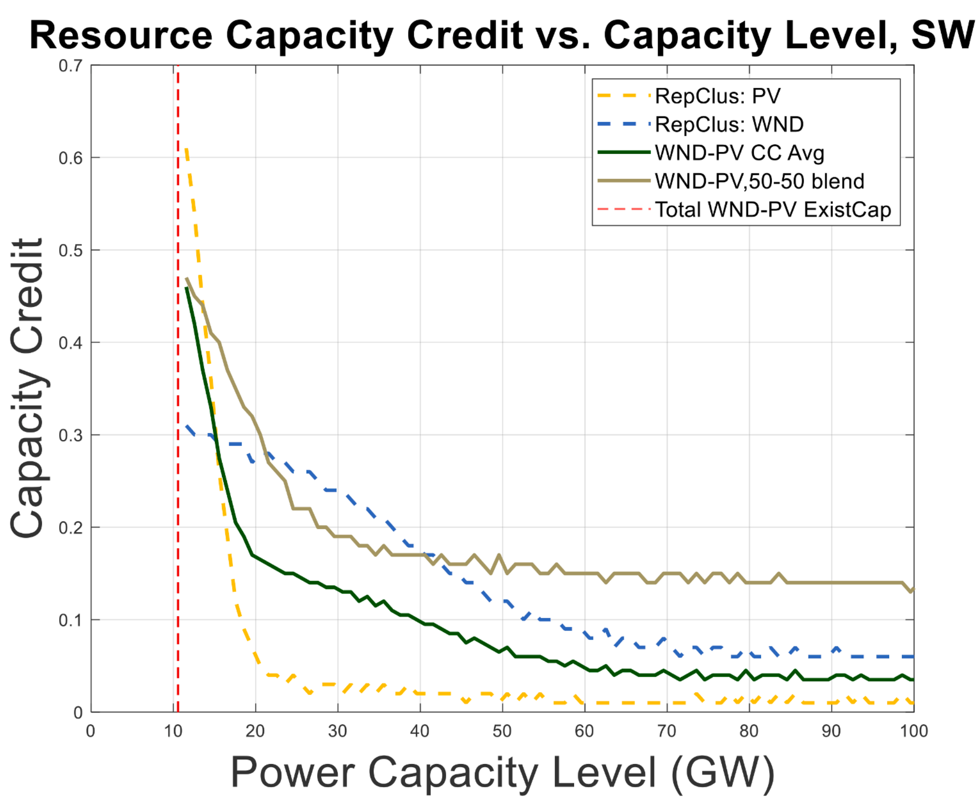

Fig. A3. Comparison of average CC from representative clusters to representative cluster blend, SW.

VRE generation data and net load data is explored. It is shown in [30] that capacity factor and capacity value show strong correlation, but only at low wind capacities. Here, an estimation method that uses the average capacity factor for the hours with the highest net load is used, under increasing penetrations of the resource.

In Fig. 3, each panel displays a set of curves that differ in the number of hours of peak net load considered. When observing the top 1-h scenario, the average capacity factor would just be the corresponding

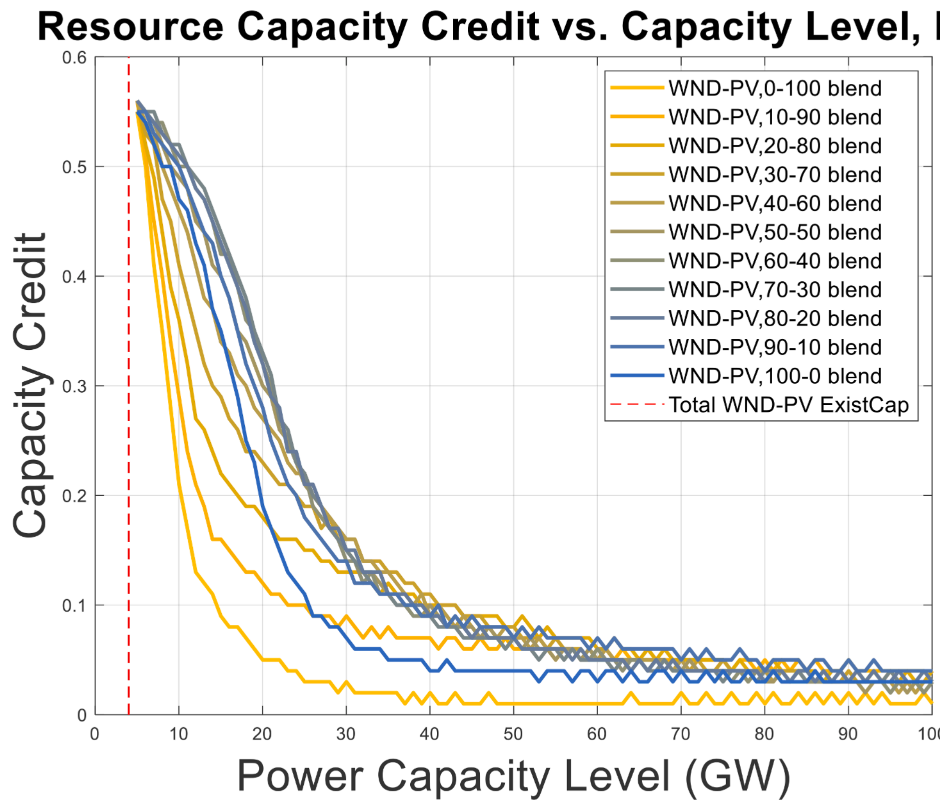

Fig. A4. Various onshore wind and solar resource mix blends from representative clusters, NE.

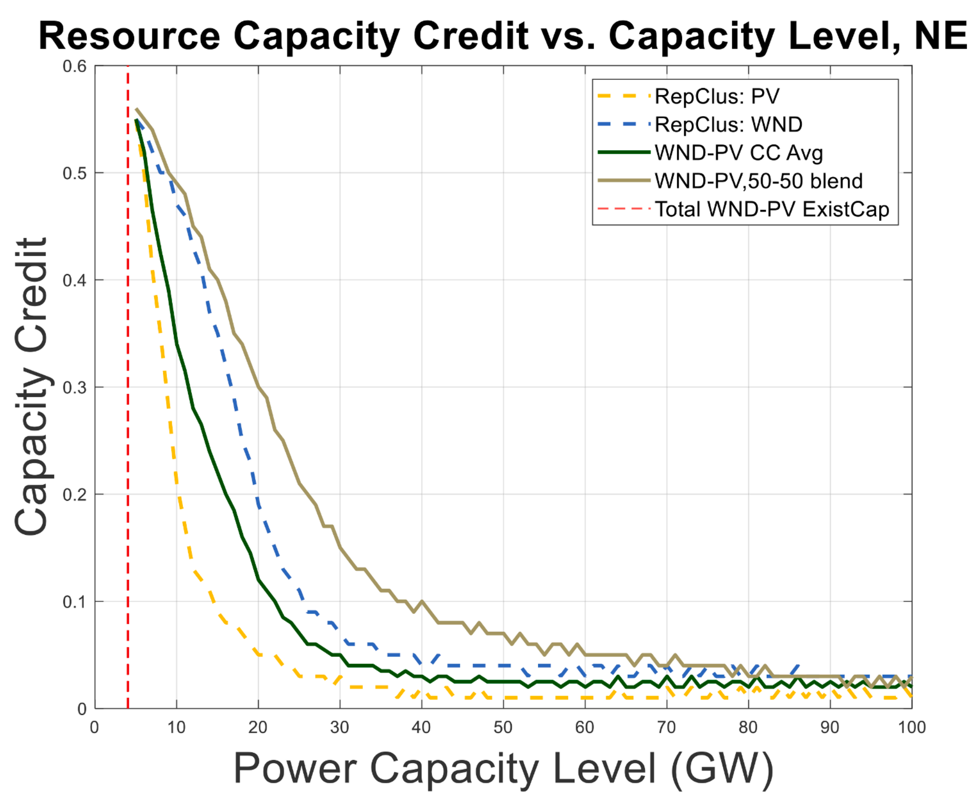

Fig. A5. Comparison of average CC from representative clusters to representative cluster blend, NE.

capacity factor for the renewable resource in the highest net demand hour. When observing the top 75-h scenario, the average capacity factor would be the mean average of capacity factors corresponding to the top 75 demand hours as increments increase. As the penetration of renewable energy increases, the hours during which the highest net load occurs changes, eventually shifting to hours during which there is little

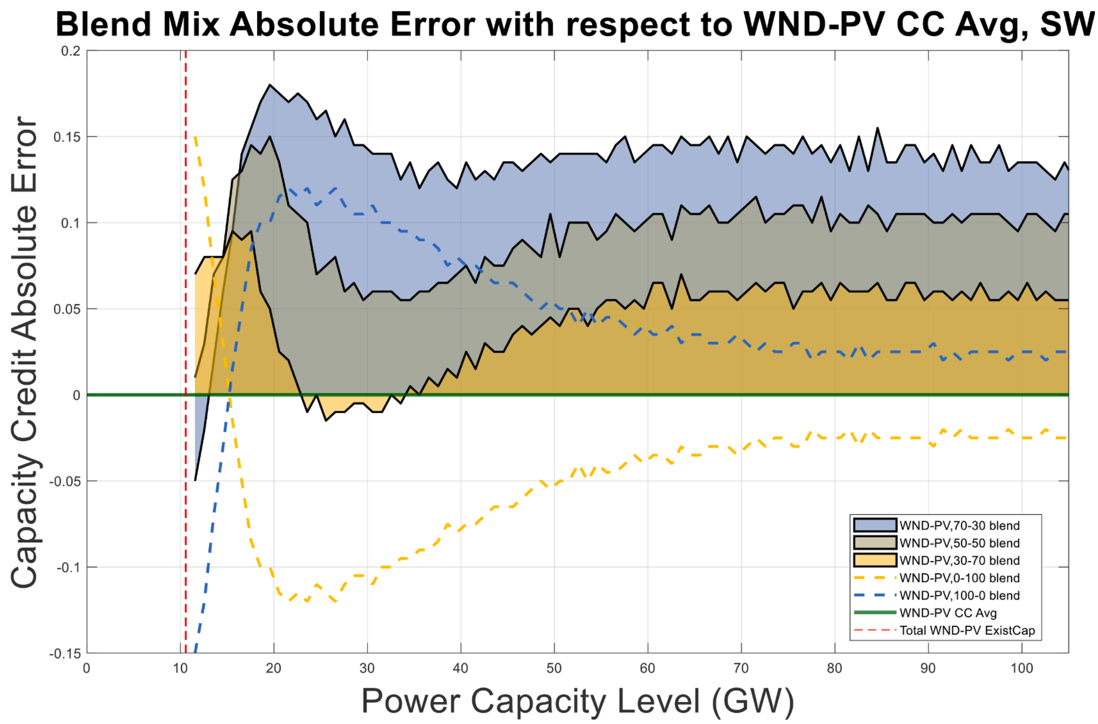

Fig. A6. WND-PV blend mix absolute error, SW.

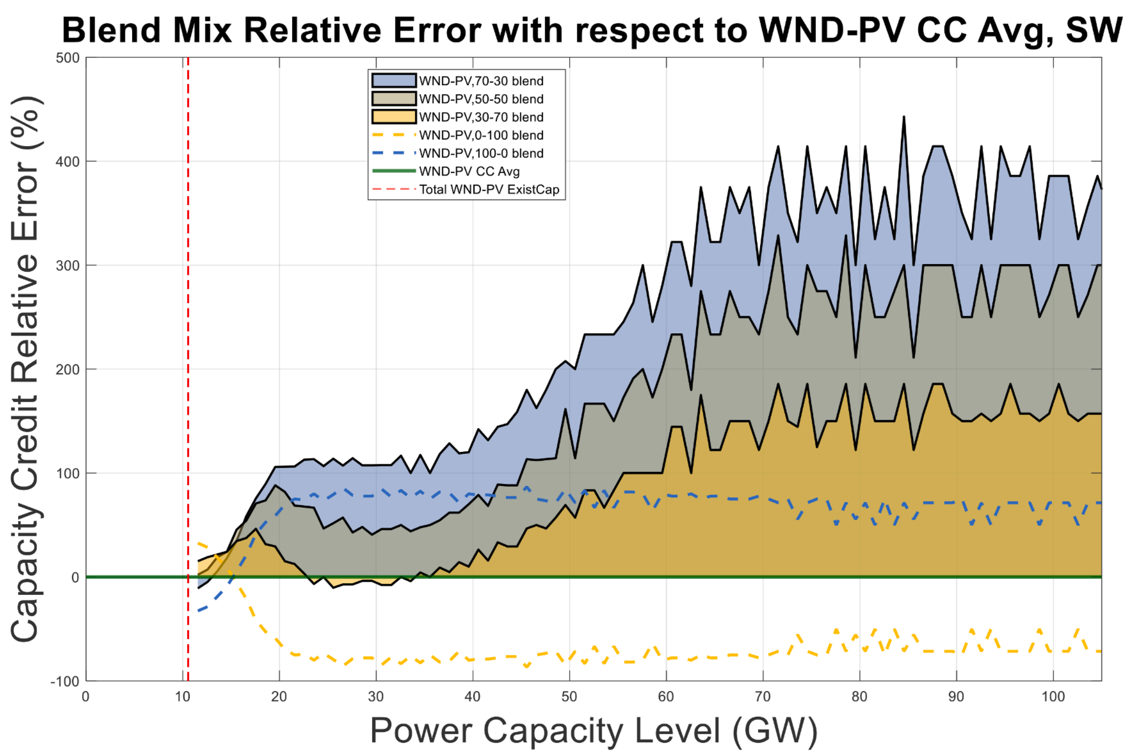

Fig. A7. WND-PV blend mix relative error, SW.

renewable generation.

Fig. 3 compares average capacity factor curves for increasing arrays of top net load hours for the NE region. As expected, decreasing average capacity factors under higher penetrations of renewables are observed and a smoothing effect occurs when more hours are considered. Note that the hours included in the simple approach are the top *net* load hours, which inherently includes the impact of previously added variable renewables. Under increasing penetrations of VREs, the highest net load hours often change, as the VRE generation pushes some, but not all, hours to lower net loads.

Similarities in the trends relative to the CC results derived from the ELCC method are seen. To understand the suitability of a capacity factor-based estimation method, results shown in Fig. 3 are compared to the CCs estimated using the full ELCC approach. Fig. 4 displays the variance

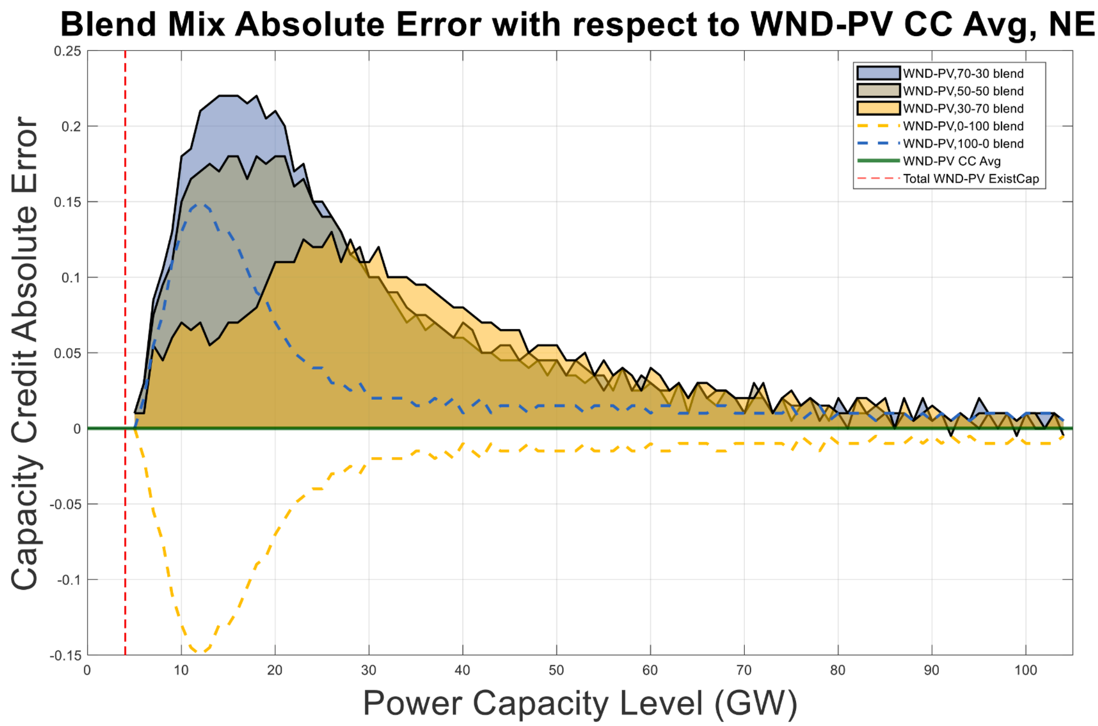

Fig. A8. WND-PV blend mix absolute error, NE.

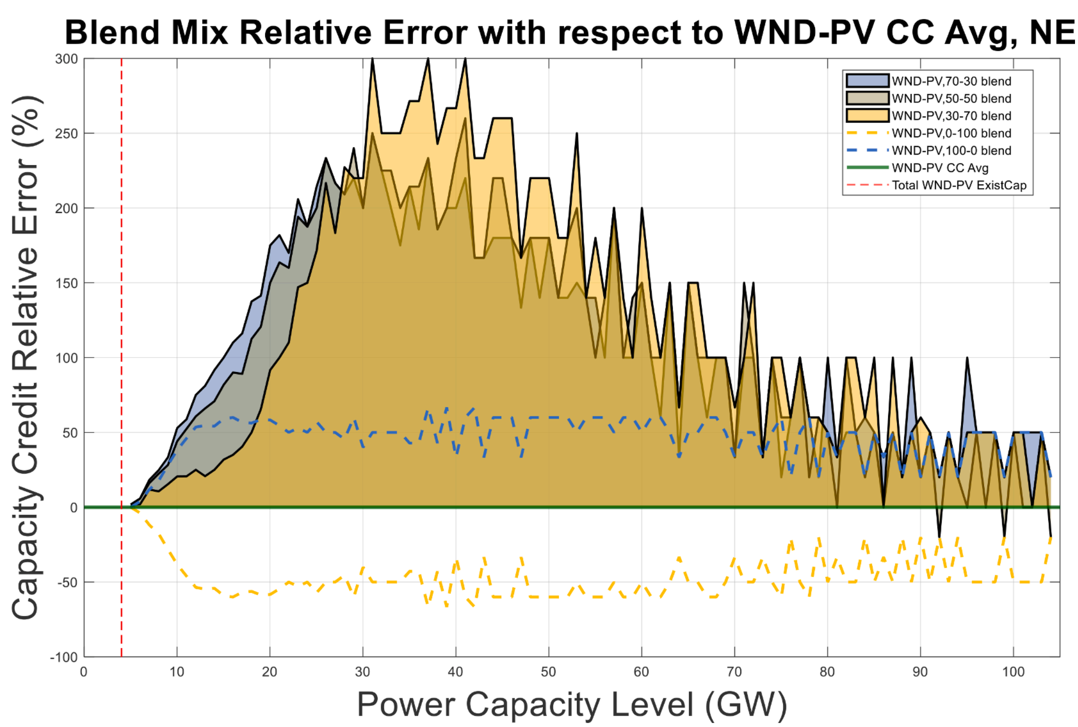

Fig. A9. WND-PV blend mix relative error, NE.

range for multiple cases when using the simple capacity factor method relative to the comparable results for the ELCC method. A relative error representation of Fig. 4 is found in the appendix.

Our results show wind and solar capacity credits can generally be estimated well by using the capacity factors of the resources in the top 1 to 25 h of net demand, with mean absolute error solved for variances below 0.05. This means that when using the estimation method for the top 1 to 25 h, the resulting estimate will be no greater than ± 0.05. A mean relative error representation is shown in the appendix.

Results differ by region, but generally the curves with the least error regardless of region or resource are those where the top 5 to 15 demand hours are used to calculate an average capacity factor CC estimate as VRE resource is incrementally added to each regional grid. Across the nine regions, the estimation method using the top 10 net load hours produced the closest results to the ELCC method, as determined by the mode of the hours with the lowest error. However, some regions, like

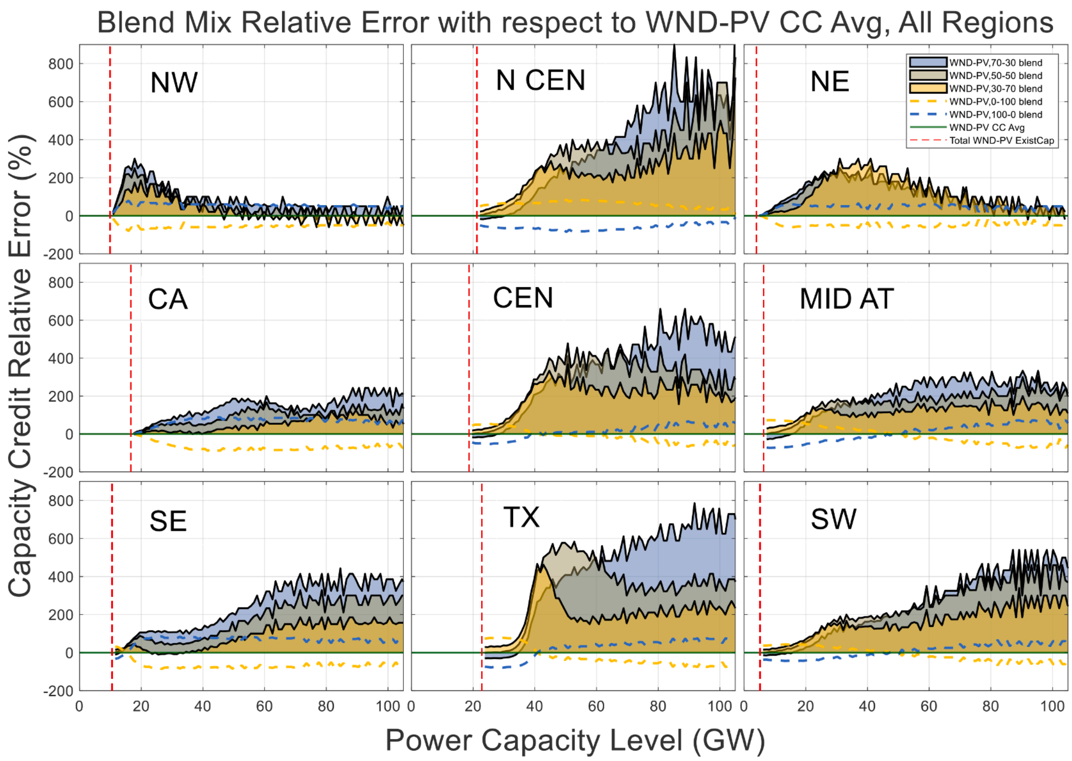

Fig. A10. WND-PV blend mix relative error, all regions.

CEN and TX, exhibit CC error minima with a greater number of top hours (50–70 hs).

3.4. Resource blending of wind and solar

One way to combat decreasing capacity value under increasing penetration of VREs is to employ resource blending. An example of this is exhibited by Chen et al. [26], through the diversification of wind farm locations and the interconnection of those sources across a large area. The homogenous resource blending of wind resources helps average out wind speed variance, thus increasing wind peak capacity. This geographic spreading can reduce wind curtailment and transmission congestion [31]. Heterogenous resource blending can yield benefits such as reduced inter-annual variability in peak net load values [32]. Diversity in VRE can boost CC values and improve grid reliability [4,33].

To explore the concept of VRE diversity further, some trials of onshore wind and solar resource blending were performed; related work shows that the two sources complement each other [1,9,17]. Fig. 5 displays capacity credit curves for various blends by percentage stake. For every new 1000 MW increment of VRE resource in a 30–70 WND-PV blend for example, 300 MW would be wind and 700 MW would be solar. Fig. 6 displays a comparison of a 50-50 WND-PV blend of representative median cluster wind and solar resources to the average CC of those resources for all regions. In every region the 50-50 blend performs better than the representative median cluster CC average.

In Fig. 7, the differences in resource blend mix CCs relative to the WND-PV CC average of the representative median clusters are displayed in absolute error plots. To express more detail, additional example region plots displaying findings in Figs. 5–7 are provided in the appendix.

4. Discussion

Our results show that CC does in fact have decreasing value as the penetration of renewables increases. VREs are an important component of many least cost decarbonization plans, but they pose new challenges in maintaining reliable operation of the grid. Given the low costs of solar and wind power, it is essential to properly attribute capacity value so that power systems build enough—but not too much—clean and firm generation when transitioning to a decarbonized system. Small underestimates in CC have little impact on system build out, but large ones can reduce VRE deployment by a significant percentage [28].

When accounting for increasing deployment of singular resource types, the proposed estimation method using average capacity factors is effective in quickly forecasting CC estimates when compared to the more computationally intensive ELCC capacity credit process.

The results from this CC credit study also show that wind and solar resource have impact on each other when blended/deployed together, in a way that is synergistic; this behavior presents rationale to account for future VRE deployment by gradual implementation of several resource types collectively, rather than focusing on the implementation of singular resource types. The proposed average capacity factor estimation method does not account for this resource blending; an effective estimation method that can account for resource blending still needs to be explored.

4.1. Study limitations & potential for supplemental work

One way to mitigate the challenges from the variability of VREs is by using energy storage, which is not accounted for in this study. There is a symbiotic effect between the use of storage and renewables, especially for solar photovoltaics. When used together, they provide more capacity value than the sum of their individual parts [14]. In the past, energy storage has been utilized for ancillary services, such as spinning reserves and frequency regulation, rather than peak shaving. However, with shorter duration net load peaks, peak shaving applications are more viable. The drop in battery prices worldwide over the last three decades has also made the future of energy storage more favorable [34]. Determining the CC of energy storage can be difficult however, as it is an energy limited and time-dependent resource. Energy storage that prevents one LOLE event may have less energy available to mitigate another LOLE event depending on load behavior [35]. Thus, a battery unit's ability to serve load at a given time depends on its prior operation [21].

Energy storage helps with shifting the hours of peak load, or the deferral of peak capacity. The shorter the discharge duration, the higher the CC of the energy storage. Batteries are also dependent on the underlying grid mix [14]. The economics of cooperative VRE and energy storage use have been investigated [36], along with strategic control of energy storage [37].

The impacts of extreme weather-related risk events and correlated generation plant failures are also not accounted for in this study. In the Monte Carlo simulations used, the probability of one particular plant's availability is independent of another plant's availability, but more realistic correlated failure simulations should be done. Some application of temperature-dependent forced outage rates (TDFOR), as seen in Murphy et al. [7], would be valuable to forming more realistic capacity credit curves than the found curves that assume all generation plants to act independently of one another when forming cumulative grid generation.

VRE implementation must also employ resilience strategies, so the grid is as operational as possible when natural disasters occur [38]. One way of improving resilience is by accounting for decentralized single unit generation from residential areas back into the grid for resources such as solar photovoltaics [39].

The found results from this CC study contribute to the understanding of resilience planning. In the future, a metric to determine best fit of average capacity factors to the reference capacity credits should be used, as it is possible that the best fitting curves can still be poorly fitted to the reference. Also, performing these studies over a longer time period than a year would be beneficial. The CC calculated in a good wind year could be double the value in a bad wind year; thus, use of more data is favorable. However, wind data for power generation is often limited [30].

5. Conclusion

In a time of decarbonization, determining the CC of VREs is vital to fully understanding how they impact the electric grid. Renewables will continue to be the fastest growing source of electricity generation through 2050 due to continuing declines in their capital costs. VREs are also supported by federal tax credits and higher state-level VRE targets across the globe. Furthermore, CC work is being done on renewable distributed generation (RDG) which has a low environmental burden. Significant reduction in carbon emissions occurs when RDG is paired with demand response (DR) in smart grids [33,40].

ELCC has and will continue to impact policy. ELCC has also been incorporated in utility commissions and government research [11,35]. In the United States, the Astrapé Strategic Energy & Risk Valuation Model (SERVM) has been used to perform ELCC analysis for utilities across the country [41]. ELCC analyses are now commonplace with respect to VRE and energy storage pairings [4,41,42].

Proper treatment of capacity credit is essential, and it is demonstrated in this study that VRE CC varies greatly by penetration and region. Utility operators and long-term capacity expansion models need to take this into account. Simple methods, like the presented approximation method, could be readily used to improve long term capacity planning.

Declaration of Competing Interest

At time of submission, Dr. Joseph DeCarolis was a full North Carolina State University employee. Starting April 11th, 2022, Dr. Joseph DeCarolis was employed by the U.S. Energy Information Administration (EIA). After acceptance of the article, Jethro Ssengonzi began an internship at the National Renewable Energy Laboratory.

Acknowledgments

The authors gratefully acknowledge the Alfred P. Sloan Foundation, the NC State University KIETS Climate Leaders Program, and the Duke University Energy Data Analytics PhD Student Fellowship (Alfred P. Sloan Foundation Grant G-2020-13922) for their financial support of the project. The authors also gratefully acknowledge the support of the Open Energy Outlook Electricity Team and Dr. Meagan Kittle-Autry for her valuable feedback.

Appendix

This appendix holds additional content referenced in previous sections.

References

[1] B. Zeng, J. Zhang, X. Yang, J. Wang, J. Dong, Y. Zhang, Integrated planning for transition to low-carbon distribution system with renewable energy generation and demand response, IEEE Trans. Power Syst. 29 (3) (2014) 1153–1165.

[2] A. Keane, et al., 'Capacity value of wind power,'', IEEE Trans. Power Syst. 26 (2) (May 2011) 564–572.

[3] C.J. Dent, R. Sioshansi, J. Reinhart, A.L. Wilson, S. Zachary, M. Lynch, C. Bothwell, C. Steele, Capacity value of solar power: report of the IEEE PES task force on capacity value of solar power, in: 2016 International Conference on Probabilistic Methods Applied to Power Systems (PMAPS), IEEE, 2016, pp. 1–7.

[4] Specht, Mark (Senior Energy Analyst), "ELCC Explained: the Critical Renewable Energy Concept You've Never Heard Of", October 12, 2020, https://blog.ucsusa.org/mark-specht/elcc-explained-the-critical-renewable-energy-concept-youve-never-heard-of/.

[5] S. Samadi and C. Singh, "Capacity credit evaluation of solar power plants," 2014 IEEE PES General Meeting | Conference & Exposition, 2014, pp. 1-5, doi:10.1109/PESGM.2014.6938831.

[6] S.H. Madaeni, R. Sioshansi, P. Denholm, Estimating the capacity value of concentrating solar power plants: a case study of the Southwestern United States, IEEE Trans. Power Syst. 27 (2) (May 2012) 1116–1124, https://doi.org/10.1109/TPWRS.2011.2179071.

[7] S. Murphy, L. Lavin, J. Apt, Resource adequacy implications of temperature-dependent electric generator availability, Appl. Energy 262 (2020), 114424.

[8] G.R. Pudaruth, F. Li, 'Locational capacity credit evaluation, IEEE Trans. Power Syst. 24 (2) (May 2009) 1072–1079.

[9] G.R. Pudaruth, F. Li, Capacity credit evaluation: a literature review, in: 2008 Third International Conference on Electric Utility Deregulation and Restructuring and Power Technologies, 2008, pp. 2719–2724, https://doi.org/10.1109/DRPT.2008.4523872.

[10] R. Perez, M. Taylor, T. Hoff, J.P. Ross, Reaching consensus in the definition of photovoltaics capacity credit in the USA: a practical application of satellite-derived solar resource data, IEEE J. Select. Topics Appl. Earth Observ. Remote Sens. 1 (1) (Mar. 2008) 28–33.

[11] An Effective Load Carrying Capability Analysis for Estimating the Capacity Value of Solar Generation Resources on the Public Service Company of Colorado System, Xcel Energy Services, Inc., Feb. 2009. https://appsrv.pace.edu/voscoe/?do=viewFullResource&resID=4277KB033016023741.

[12] I. Bromley-Dulfano, J. Florez, M.T. Craig, Reliability benefits of wide-area renewable energy planning across the Western United States, Renew. Energy 179 (2021) 1487–1499.

[13] H. Kim, R. Sioshansi, E. Lannoye and E. Ela, "A stochastic-dynamic-optimization approach to estimating the capacity value of energy storage," in IEEE Trans. Power Syst., doi:10.1109/TPWRS.2021.3110497.

[14] D. Sodano, J. DeCarolis, J.X. Johnson, A.R. de Queiroz, The symbiotic relationship of solar power and energy storage in providing capacity value, Renew. Energy (2021), https://doi.org/10.1016/j.renene.2021.05.122.

[15] P. Brown, "Patrickbrown4/Zephyr: ZERO-emissions electricity system planning with hourly operational resolution," GitHub. [Online]. Available: https://github.com/patrickbrown4/zephyr. [Accessed: 07-Apr-2022].

[16] B. Zeng, X. Wei, B. Sun, F. Qiu, J. Zhang, X. Quan, Assessing capacity credit of demand response in smart distribution grids with behavior-driven modeling framework, Int. J. Electr. Power Energy Syst. 118 (2020 Jun 1), 105745.

[17] J. Feng, B. Zeng, D. Zhao, G. Wu, Z. Liu, J. Zhang, Evaluating demand response impacts on capacity credit of renewable distributed generation in smart distribution systems, IEEE Access 6 (2017 Sep 11) 14307–14317.

[18] Open energy outlook for the United States, https://github.com/TemoaProject/oeo, https://openenergyoutlook.org/, https://github.com/TemoaProject/oeo/blob/master/OEO_Roadmap.md.

[19] E. Tómasson, L. Söder, Multi-area generation adequacy and capacity credit in power system analysis, in: 2017 IEEE Innovative Smart Grid Technologies-Asia (ISGT-Asia), IEEE, 2017, pp. 1–6. Dec 4.

[20] M. Milligan, National Renewable Energy Laboratory, K. Porter, Exeter Associates, Inc., "Determining the Capacity Value of Wind: An Updated Survey of Methods and Implementation Preprint ", To be presented at WindPower 2008 Houston, Texas June 1–4, 2008, https://www.nrel.gov/docs/fy08osti/43433.pdf.

[21] R. Sioshansi, S. Hossein Madaeni, P. Denholm, A dynamic programming approach to estimate the capacity value of energy storage, IEEE Trans. Power Syst. 29 (1) (2013) 395–403.

[22] North American Electric Reliability Corporation, EFORd data from 2018, "Methods to Model and Calculate Capacity Contributions of Variable Generation for Resource Adequacy Planning", North American Electric Reliability Corporation, Princeton, NJ, USA, Mar. 2011. https://www.nrel.gov/docs/fy11osti/51485.pdf.
[23] PowerGenome, "PowerGenome/PowerGenome: a tool to quickly and easily create inputs for power systems models," GitHub. [Online]. Available: https://github.com/PowerGenome/PowerGenome. [Accessed: 07-Apr-2022].
[24] U.S. Energy Information Administration https://www.eia.gov/electricity/gridmonitor/dashboard/electric_overview/US48/US48.
[25] A. Reimers, W. Cole, B. Frew, The impact of planning reserve margins in long-term planning models of the electricity sector, Energy Policy 125 (2019) 1–8.
[26] J. Chen, L. Feng, Using lower and upper bounds to increase the computing accuracy of Monte Carlo method, in: 2010 International Conference on Computational and Information Sciences, 2010, pp. 630–633, https://doi.org/10.1109/ICCIS.2010.159.
[27] R. Heijungs, On the number of Monte Carlo runs in comparative probabilistic LCA, Int. J. Life Cycle Assess. 25 (2020) 394–402. https://doi-org.prox.lib.ncsu.edu/10.1007/s11367-019-01698-4.
[28] E. Zhou, W. Cole, B. Frew, Valuing variable renewable energy for peak demand requirements, Energy 165 (2018) 499–511.
[29] M. Amelin, Comparison of capacity credit calculation methods for conventional power plants and wind power, IEEE Trans. Power Syst. 24 (2) (May 2009) 685–691.
[30] B. Hasche, A. Keane, M. O'Malley, Capacity value of wind power, calculation, and data requirements: the Irish power system case, IEEE Trans. Power Syst. 26 (1) (2011) 420–430.
[31] J. Novacheck, J. Johnson, Diversifying wind power in real power systems, Renew. Energy (2017) 106, https://doi.org/10.1016/j.renene.2016.12.100.
[32] T.H. Ruggles, K. Caldeira, Wind and solar generation may reduce the inter-annual variability of peak residual load in certain electricity systems, Appl. Energy 305 (2022), 117773.
[33] Y. Zhang and S. Ula, "Estimation of wind power availability and capacity credit for multiple wind farms," 41st North American Power Symposium, 2009, pp. 1-5, doi:10.1109/NAPS.2009.5484008.
[34] H. Ritchie, The price of batteries has declined by 97% in the last three decades, Our World in Data (2021), 04-Jun-[Online]. Available: https://ourworldindata.org/battery-price-decline [Accessed: 02-Aug-2022].
[35] M. Brown, W.J. Cole, K.P. Eurek, J. Becker, D.A. Bielen, I. Chernyakhovskiy, S. M. Cohen, A. Frazier, P.J. Gagnon, N. Gates, D. Greer, Regional energy deployment system (ReEDS) model documentation: version 2019, Natl. Renew. Energy Lab. (NREL) (2020). Mar 24.
[36] Y. Xu, C. Singh, Adequacy and economy analysis of distribution systems integrated with electric energy storage and renewable energy resources, IEEE Trans. Power Syst. 27 (4) (2012) 2332–2341.
[37] N. Shi, Y. Luo, Capacity value of energy storage considering control strategies, PloS one 12 (5) (2017), e0178466. May 30.
[38] "2021Lecture01_Introduction_v5.pdf", Dr Ning Lu ECE 451 Class Notes Fall 2021.
[39] "LA100: The Los Angeles 100% Renewable Energy Study Executive Summary - NREL." [Online]. Available: https://www.nrel.gov/docs/fy21osti/79444-ES.pdf. [Accessed: 12-May-2022].
[40] Y. Zhou, P. Mancarella, J. Mutale, 'Framework for capacity credit assessment of electrical energy storage and demand response,'', IET Generat., Transmiss. Distrib. 10 (9) (2016) 2267–2276.
[41] ELCCs rules at other ISOs-RTOs, Andrew Levitt, Applied Innovation April 7, PJM Capacity Capability Senior Task Force (2020). https://www.pjm.com/-/media/committees-groups/task-forces/ccstf/2020/20200407/20200407-item-05-elcc-at-otherisortos.ashx.
[42] Duke Energy Progress, Integrated Resource Plan Attachment IV, 2020 Duke Energy Carolinas And Duke Energy Progress Storage Effective Load Carrying Capability (ELCC) Study, https://starw1.ncuc.net/NCUC/ViewFile.aspx?Id=2ea3a3fd-1613-4b1d-babd-cb328b7a27e7.